

Quaternion-Based Impedance Control for Dual-Robot Cooperation

Fabrizio Caccavale, Ciro Natale, Bruno Siciliano, Luigi Villani

PRISMA Lab

Dipartimento di Informatica e Sistemistica

Università degli Studi di Napoli Federico II

Via Claudio 21, 80125 Napoli, Italy

{caccaval,cinatale,siciliano,lvillani}@unina.it

Abstract

A quaternion-based impedance control framework is presented which ensures geometric consistency for the execution of six-DOF interaction tasks. This is applied to cooperative manipulation of an object by two robots. Both loose and tight cooperative control schemes are designed, and the theoretical findings are validated in experiments on a dual-robot industrial setup.

1. Historical Overview and Introduction

Impedance control [1] is a well-established framework to manage the interaction with the environment of an object manipulated by a robotic system. A prescribed dynamic behavior in terms of mass, damping and stiffness can be imposed between end-effector displacements and contact forces. According to this strategy, an indirect force control is achieved which is effective even when the end effector is in contact with an unstructured environment [2].

The approach may yield some drawbacks for the execution of six-DOF tasks since the rotational part of the impedance is not well defined when using a minimal representation of orientation. Representation singularities occur if a minimal description of end-effector orientation is used, e.g., with the operational space framework [3]. Further, task geometric inconsistency may arise due to dependence of the rotational stiffness upon the actual object orientation. A spatial impedance concept has been recently proposed based on an energy formulation using rotation matrices [4]. Based on this approach, a class of geometrically meaningful angle/axis representations to describe orientation displacements has been introduced which comprises the unit quaternion [5].

Whenever object manipulation requires the adoption of more than a single robot, it is necessary to manage

cooperation between multiple robots. Cooperative manipulation constitutes an effective way to execute complex robotic tasks. To this purpose, it is worth distinguishing between loose cooperation and tight cooperation. The former is accomplished at the task planning level [6, 7], e.g., in coordinated workcell tasks, assembly. The latter, instead, is realized at both task planning and control level [8, 9], e.g., in carrying heavy objects, grasping. Solutions to the problem of object manipulation include the symmetric formulation in [10], the object level framework in [11] and the impedance control of internal forces in [12]. On the other hand, the problem of object interaction with the environment has been tackled in [13] and [14].

This paper is aimed at presenting a geometrically consistent quaternion-based impedance control framework and showing its potential in a dual-robot cooperative manipulation context. Both loose and tight cooperation are considered. In the former the two robots are independently controlled and cooperation is realized only at the task planning level, whereas in the latter the two robots are controlled in a coordinated fashion. Experimental results on a dual-robot industrial setup are discussed for a typical parts mating task and for a task where a tightly grasped object interacts with the environment.

2. Quaternion-Based Impedance

Consider a rigid object in contact with the environment. In order to describe the interaction, it is worth defining a frame Σ_o attached to the object; its origin and orientation with respect to the base frame Σ_b are characterized by the (3×1) position vector p_o and the (3×3) rotation matrix R_o , respectively. Hereafter, a superscript will denote the frame to which a quantity is referred; when referred to the base frame, the super-

script will be dropped.

Typically, a desired frame Σ_d is assigned in terms of \mathbf{p}_d and \mathbf{R}_d . Further, a mechanical impedance can be introduced which is aimed at imposing a suitable dynamic behavior for the position and orientation displacements between the desired frame Σ_d and a compliant frame Σ_c characterized by \mathbf{p}_c and \mathbf{R}_c . The mutual position between Σ_d and Σ_c can be described by the position displacement vector

$$\Delta \mathbf{p}_{dc} = \mathbf{p}_d - \mathbf{p}_c, \quad (1)$$

which has been referred to Σ_b .

The impedance equation is typically chosen so as to impose a dynamic behavior for the position displacement under a (3×1) force vector \mathbf{f}_o at the object, i.e.,

$$\mathbf{M}_p \Delta \ddot{\mathbf{p}}_{dc} + \mathbf{D}_p \Delta \dot{\mathbf{p}}_{dc} + \mathbf{K}_p \Delta \mathbf{p}_{dc} = \mathbf{f}_o, \quad (2)$$

where \mathbf{M}_p , \mathbf{D}_p and \mathbf{K}_p are (3×3) positive definite matrices representing the mass, damping, and stiffness characterizing the impedance.

The stiffness matrix \mathbf{K}_p can be decomposed as

$$\mathbf{K}_p = \mathbf{U}_p \mathbf{\Gamma}_p \mathbf{U}_p^T, \quad (3)$$

where $\mathbf{\Gamma}_p = \text{diag}\{\gamma_{p1}, \gamma_{p2}, \gamma_{p3}\}$ is the eigenvalue matrix and $\mathbf{U}_p = [\mathbf{u}_{p1} \ \mathbf{u}_{p2} \ \mathbf{u}_{p3}]$ is the eigenvector matrix. Considering a position displacement of length λ along the i -th eigenvector leads to

$$\mathbf{K}_p \Delta \mathbf{p}_{dc} = \gamma_{pi} \lambda \mathbf{u}_{pi} \quad (4)$$

which represents an elastic force along the same \mathbf{u}_{pi} axis. This implies that the translational stiffness matrix can be expressed in terms of three parameters γ_{pi} representing the stiffness along three principal axes \mathbf{u}_{pi} , and in turn it allows the translational stiffness to be specified in a consistent way with the task geometry [4].

In the classical six-DOF approaches, the rotational part of the impedance equation is defined by extending the formal expression of the equation written for the translational part (2) and using a minimal representation of end-effector orientation in terms of three Euler angles. By adopting an algebraic difference analogous to that used for the position displacement in (1), the orientation displacement can be computed as

$$\Delta \phi_{dc} = \phi_d - \phi_c \quad (5)$$

where ϕ_d and ϕ_c denote the set of Euler angles corresponding to \mathbf{R}_d and \mathbf{R}_c , respectively. Then, the rotational part of the impedance at the end effector can be defined as

$$\mathbf{M}_\phi \Delta \ddot{\phi}_{dc} + \mathbf{D}_\phi \Delta \dot{\phi}_{dc} + \mathbf{K}_\phi \Delta \phi_{dc} = \mathbf{T}^T(\phi_c) \boldsymbol{\mu}_o, \quad (6)$$

where \mathbf{M}_ϕ , \mathbf{D}_ϕ , \mathbf{K}_ϕ are positive definite matrices describing the generalized inertia, rotational damping, rotational stiffness, respectively, and $\boldsymbol{\mu}_o$ is the contact moment at the end effector; all the above quantities have been referred to the base frame, and $\mathbf{T}^T(\phi_c)$ is the transformation matrix needed to express the moment in terms of an equivalent operational space quantity, via a kineto-static duality concept based on the relationship $\boldsymbol{\omega}_c = \mathbf{T}(\phi_c) \dot{\phi}_c$.

Notice that, differently from (2), the dynamic behavior for the rotational part is not merely determined by the choice of the impedance parameters but it does also depend on the orientation of the compliant frame with respect to the base frame through the matrix $\mathbf{T}^T(\phi_c)$. Moreover, Equation (6) becomes ill-defined in the neighborhood of a representation singularity; in particular, at such a singularity, moment components in the null space of \mathbf{T}^T do not generate any contribution to the dynamics of the orientation displacement, leading to a possible build-up of large values of contact moment.

A simple inspection of the resulting elastic moment $\mathbf{T}^{-T}(\phi_c) \mathbf{K}_\phi \Delta \phi_{dc}$ from (6) reveals that, even in the absence of representation singularities, a decomposition of \mathbf{K}_ϕ analogous to (3) does not allow the eigenvectors of \mathbf{K}_ϕ to represent the three principal axes of the rotational stiffness. It can be concluded that the property of task geometric consistency is lost.

A solution to this problem has been proposed in [5], where a class of geometrically meaningful representations of the mutual orientation between the desired frame and the compliant frame is considered. In detail, the rotation matrix describing the orientation of Σ_d with respect to Σ_c can be expressed in terms of the (3×3) rotation matrix

$${}^c \mathbf{R}_d = {}^c \mathbf{r}_{dc} {}^c \mathbf{r}_{dc}^T + (\mathbf{I} - {}^c \mathbf{r}_{dc} {}^c \mathbf{r}_{dc}^T) \cos \vartheta_{dc} + \mathbf{S}({}^c \mathbf{r}_{dc}) \sin \vartheta_{dc}, \quad (7)$$

where an equivalent rotation by an angle ϑ_{dc} about an axis with (3×1) unit vector ${}^c \mathbf{r}_{dc}$ has been considered, \mathbf{I} is the (3×3) identity matrix, and $\mathbf{S}(\cdot)$ is the (3×3) skew-symmetric matrix operator performing the cross product between two (3×1) vectors.

A convenient singularity-free representation of the orientation displacement is given by the unit quaternion $\mathcal{Q}_{dc} = \{\eta_{dc}, {}^c \boldsymbol{\epsilon}_{dc}\}$ defined as

$$\eta_{dc} = \cos \frac{\vartheta_{dc}}{2} \quad (8)$$

$${}^c \boldsymbol{\epsilon}_{dc} = \sin \frac{\vartheta_{dc}}{2} {}^c \mathbf{r}_{dc}. \quad (9)$$

Note that $\{\eta_{dc}, {}^c \boldsymbol{\epsilon}_{dc}\}$ and $\{-\eta_{dc}, -{}^c \boldsymbol{\epsilon}_{dc}\}$ represent the same orientation; also, Σ_d is aligned with Σ_c as long as $\eta_{dc} = \pm 1$ and ${}^c \boldsymbol{\epsilon}_{dc} = \mathbf{0}$.

Let M_ϵ , D_ϵ , K_ϵ denote (3×3) positive definite matrices representing the inertia, rotational damping, and rotational stiffness. Then, the impedance equation for the orientation displacement under a (3×1) moment vector μ_o with respect to the origin of Σ_o is given by

$$M_\epsilon \Delta^c \dot{\omega}_{dc} + D_\epsilon \Delta^c \omega_{dc} + K'_\epsilon \epsilon_{dc} = {}^c \mu_o, \quad (10)$$

where $\Delta^c \omega_{dc} = {}^c \omega_d - {}^c \omega_c$ is the (3×1) angular velocity vector of Σ_d relative to Σ_c , and K'_ϵ is an equivalent stiffness which is related to K_ϵ as

$$K'_\epsilon = 2(\eta_{dc} I + S({}^c \epsilon_{dc})) K_\epsilon. \quad (11)$$

The relationship between K'_ϵ and K_ϵ can be investigated by considering the decomposition of K_ϵ as

$$K_\epsilon = U_\epsilon \Gamma_\epsilon U_\epsilon^T, \quad (12)$$

where $\Gamma_\epsilon = \text{diag}\{\gamma_{\epsilon 1}, \gamma_{\epsilon 2}, \gamma_{\epsilon 3}\}$ is the eigenvalue matrix and $U_\epsilon = [u_{\epsilon 1} \ u_{\epsilon 2} \ u_{\epsilon 3}]$ is the eigenvector matrix. An orientation displacement $\{\cos(\vartheta_{dc}/2), \sin(\vartheta_{dc}/2)u_{\epsilon i}\}$ about the i -th eigenvector leads to

$$K'_\epsilon {}^c \epsilon_{dc} = \gamma_{\epsilon i} \sin \vartheta_{dc} u_{\epsilon i} \quad (13)$$

which represents an elastic moment about the same $u_{\epsilon i}$ axis. This implies that the rotational stiffness matrix K_ϵ can be expressed in terms of three parameters $\gamma_{\epsilon i}$ representing the stiffness about three principal axes $u_{\epsilon i}$, and in turn it allows the rotational stiffness to be specified in a consistent way with the task geometry.

Notice that, differently from (2), the rotational part of the impedance equation (10) has been derived in terms of quantities all referred to the compliant frame Σ_c ; this allows the impedance behavior to be effectively expressed in terms of the relative orientation of Σ_d with respect to Σ_c , no matter what the absolute orientation of Σ_c with respect to Σ_b is.

A generalization of the six-DOF quaternion-based impedance concept to the case of a nondiagonal stiffness which may be useful for certain interaction tasks can be found in [15].

3. Loose Cooperative Control

Consider a system of two robots manipulating an object. A cooperative control strategy can be termed loose when the manipulation task is executed by controlling the two robots in an independent fashion. Cooperation is realized only at the task planning level.

A typical task requiring loose cooperative control is constituted by mating rigid parts such as dual-robot assembly in a workcell. The archetype is the classical peg-in-hole, where one robot carries the peg and the

other holds the hollow part. It should be clear that the task is successfully executed provided that mating forces are suitably reduced during the insertion so as to avoid undesirable jamming and wedging. This concept can be brought to fruition by resorting to special mechanical devices such as the Remote Center of Compliance in [16] or the compliant end effectors in [17, 18].

An alternative strategy is to assign complementary roles to the two robots, i.e., to operate one robot using pure positional control while controlling the other so as to achieve a programmable impedance at the end effector. In detail, the motion of the position controlled robot is planned to match the nominal requirements of the assigned task, while the active compliant behavior imposed to the impedance controlled robot is devoted to mitigating the effects of imperfect knowledge of the task geometry and unavoidable tracking errors. The position controlled robot can be operated using the standard industrial control unit, i.e., by exploiting the set of motion planning instructions of the native programming language.

On the other hand, assuming that an open control architecture is available for the other robot, an impedance control is realized at the end-effector level where the object is either the peg or the hollow part; the end-effector frame of such a robot coincides with the object frame. According to the well-known inverse dynamics strategy [19], the joint driving torques for the impedance-controlled robot—assumed to have six joints—are chosen as

$$\tau = B(q)J^{-1}(q)(a_o - \dot{J}(q, \dot{q})\dot{q}) + n(q, \dot{q}) + J^T(q)h_o, \quad (14)$$

where q is the (6×1) vector of joint variables, B is the (6×6) positive definite and symmetric inertia matrix, n is the (6×1) vector of Coriolis, centrifugal and gravity terms, J is the (6×6) nonsingular manipulator geometric Jacobian matrix, and $h_o = [f_o^T \ \mu_o^T]^T$ is the (6×1) vector of generalized forces acting on the object. Moreover, $a_o = [a_p^T \ a_e^T]^T$ in (14) is the (6×1) vector of resolved acceleration at the end effector which is designed to match the desired impedance in (2) and (10), i.e.,

$$a_p = \ddot{p}_c + k_{vp}\Delta\dot{p}_{co} + k_{pp}\Delta p_{co} \quad (15)$$

$$a_e = \dot{\omega}_c + k_{ve}\Delta\omega_{co} + k_{pe}\epsilon_{co} \quad (16)$$

where $\Delta p_{co} = p_c - p_o$ is the position error between the origins of Σ_c and Σ_o , while ϵ_{co} is the vector part of the quaternion expressing the orientation error between Σ_c and Σ_o ; $\Delta\omega_{co} = \omega_c - \omega_o$ is the relative angular velocity. The translational and rotational impedance equations (2) and (10) are integrated, with input f_o and μ_o , to compute \ddot{p}_c and $\dot{\omega}_c$, \dot{p}_c and ω_c , and then p_c and Q_c via the quaternion propagation [20].

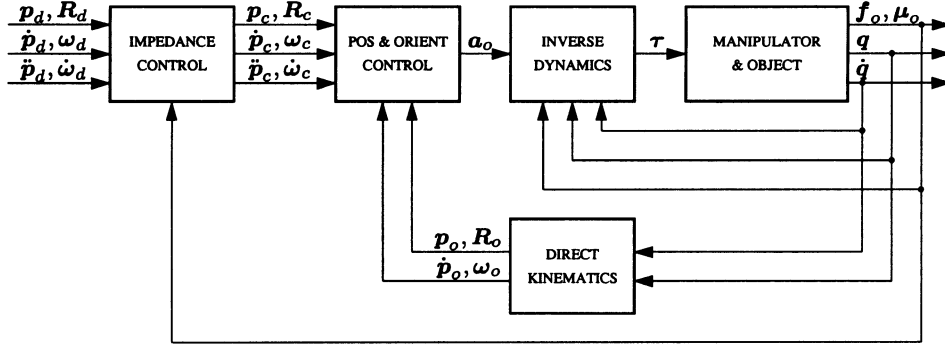


Figure 1: Six-DOF impedance control with inner position and orientation loops.

Further, k_{Vp} , k_{Pp} in (15) and $k_{V\epsilon}$, $k_{P\epsilon}$ in (16) are suitable positive feedback gains characterizing inner position and orientation loops, which can be set independently of the impedance parameters so as to provide accurate position tracking and good robustness to unmodeled dynamics and external disturbances.

A block diagram illustrating the overall impedance control scheme is sketched in Fig. 1. If desired, in the case of a redundant manipulator, a redundancy resolution technique can be nicely incorporated into the scheme by resorting to a dynamically consistent pseudoinverse of the Jacobian, as discussed in [21].

4. Tight Cooperative Control

A cooperative control strategy can be termed tight when the manipulation task is executed by controlling the two robots in a coordinated fashion. Cooperation is realized not only at the task planning level, but also at the control level. This is the typical task of two robots whose end effectors tightly grasp a commonly held rigid object, thus creating a closed-kinematic chain. In such a case, the object motion must be related to the motions of the end effectors of the two robots. This can be done by resorting to the task-oriented formulation for coordinated motion of dual-robot systems developed in [22].

Consider a system of two manipulators. For each manipulator ($k = 1, 2$) let Σ_k denote a frame attached to the end effector; its origin and orientation are characterized by the (3×1) position vector p_k and the (3×3) rotation matrix R_k , respectively. Then, $Q_k = \{\eta_k, \epsilon_k\}$ represents the unit quaternion corresponding to R_k . Let also $v_k = [\dot{p}_k^T \ \omega_k^T]^T$ be the (6×1) end-effector (linear and angular) velocity vector. All the quantities are expressed in the common base frame Σ_b .

The object position can be defined as

$$p_o = \frac{1}{2}(p_1 + p_2), \quad (17)$$

while the rotation matrix defining the orientation of Σ_o is given by

$$R_o = R_1^{-1} R^{(1}r_{21}, \vartheta_{21}/2), \quad (18)$$

where ${}^1r_{21}$ and ϑ_{21} are respectively the unit vector and the angle that realize the rotation described by

$${}^1R_2 = R_1^T R_2 \quad (19)$$

and ${}^1R^{(1}r_{21}, \vartheta_{21}/2)$ is the rotation matrix corresponding to a rotation of $\vartheta_{21}/2$ about the axis ${}^1r_{21}$.

Then the absolute orientation can be expressed as

$$Q_o = Q_1 * \left\{ \cos \frac{\vartheta_{21}}{4}, \sin \frac{\vartheta_{21}}{4} {}^1r_{21} \right\} \quad (20)$$

where Q_o is the unit quaternion corresponding to R_o and “ $*$ ” denotes the quaternion product [20]; the second factor on the right-hand side of (20) is the unit quaternion extracted from ${}^1R^{(1}r_{21}, \vartheta_{21}/2)$.

From (17) and (18), the object linear velocity \dot{p}_o and angular velocity ω_o can be expressed as

$$v_o = \frac{1}{2}(v_1 + v_2) \quad (21)$$

where $v_o = [\dot{p}_o^T \ \omega_o^T]^T$.

Let f_k and μ_k ($k = 1, 2$) respectively denote the (3×1) end-effector force and moment vectors for either manipulator. Then, according to the kineto-statics duality concept [10] applied to (21), the object force and moment can be expressed as

$$h_o = h_1 + h_2 \quad (22)$$

where $h_k = [f_k^T \ \mu_k^T]^T$ and $h_o = [f_o^T \ \mu_o^T]^T$.

In order to fully describe a coordinated motion, the position and orientation of one manipulator relative to

the other is also of concern. The mutual position between the two end effectors is defined as the vector

$$\Delta \mathbf{p}_{21} = \mathbf{p}_2 - \mathbf{p}_1. \quad (23)$$

The mutual orientation between the two end effectors is defined with reference to Σ_1 in terms of the rotation matrix ${}^1\mathbf{R}_2$, and then in terms of the quaternion product

$$\mathcal{Q}_{21} = \mathcal{Q}_1^{-1} * \mathcal{Q}_2, \quad (24)$$

where $\mathcal{Q}_1^{-1} = \{\eta_1, -\epsilon_1\}$ is the unit quaternion corresponding to \mathbf{R}_1^T .

From (23) and (19), the mutual velocity can be expressed as

$$\Delta \mathbf{v}_{21} = \mathbf{v}_2 - \mathbf{v}_1. \quad (25)$$

A control strategy for tight cooperative manipulation of an object interacting with the environment can be devised as follows. Two individual controllers are developed which guarantee tracking of a reference end-effector position $\mathbf{p}_{r,k}$ and orientation $\mathcal{Q}_{r,k}$, as well as of a reference end-effector velocity $\mathbf{v}_{r,k}$ ($k = 1, 2$). Such a reference is generated with a twofold objective; namely, realizing an impedance behavior at the object level, while assigning a mutual position and orientation between the two end effectors that is compatible with the object geometry.

The first objective can be fulfilled as follows. Let the desired object position \mathbf{p}_d and orientation \mathcal{Q}_d (extracted from \mathbf{R}_d) be assigned with the associated linear and angular velocities and accelerations. Also, the object force and moment can be computed from (22) with the end-effector forces and moments available from the wrist force/torque sensors. Then, the translational and rotational impedance equations (2) and (10) are integrated, with input \mathbf{f}_o and $\boldsymbol{\mu}_o$, to compute $\ddot{\mathbf{p}}_c$ and $\dot{\boldsymbol{\omega}}_c$, $\dot{\mathbf{p}}_c$ and $\boldsymbol{\omega}_c$, and then \mathbf{p}_c and \mathcal{Q}_c via the quaternion propagation [20].

The second objective can be fulfilled by assigning a reference mutual position $\Delta \mathbf{p}_{r,21}$ and orientation $\mathcal{Q}_{r,21}$. In particular, $\Delta \mathbf{p}_{r,21}$ and $\mathcal{Q}_{r,21}$ are taken as constant and equal to the initial values of $\Delta \mathbf{p}_{21}$ in (23) and \mathcal{Q}_{21} extracted from (19), respectively, that can be computed via the direct kinematics of the two manipulators.

The two objectives are combined by choosing the reference position and orientation for the two end effectors so as to satisfy (17), (23), (20), (24), i.e.,

$$\mathbf{p}_{r,1} = \mathbf{p}_c - \frac{1}{2} \Delta \mathbf{p}_{r,21} \quad (26)$$

$$\mathbf{p}_{r,2} = \mathbf{p}_c + \frac{1}{2} \Delta \mathbf{p}_{r,21} \quad (27)$$

$$\mathcal{Q}_{r,1} = \mathcal{Q}_c * \left\{ \cos \frac{\vartheta_{r,21}}{4}, -\sin \frac{\vartheta_{r,21}}{4} \mathbf{r}_{r,21} \right\} \quad (28)$$

$$\mathcal{Q}_{r,2} = \mathcal{Q}_{r,1} * \mathcal{Q}_{r,21}. \quad (29)$$

Further, the reference velocities for the two end effectors are chosen as

$$\mathbf{v}_{r,1} = \mathbf{v}_c - \frac{1}{2} \Delta \mathbf{v}_{r,21} \quad (30)$$

$$\mathbf{v}_{r,2} = \mathbf{v}_c + \frac{1}{2} \Delta \mathbf{v}_{r,21} \quad (31)$$

where $\mathbf{v}_c = [\dot{\mathbf{p}}_c^T \ \dot{\boldsymbol{\omega}}_c^T]^T$. Then, the reference accelerations can be computed via a time derivative of the terms in (30), (31).

The above reference trajectories can be tracked by resorting to an inverse dynamics strategy. The joint driving torques for the two robots can be chosen as ($k = 1, 2$)

$$\boldsymbol{\tau}_k = \mathbf{B}_k(\mathbf{q}_k) \mathbf{J}_k^{-1}(\mathbf{q}_k) (\mathbf{a}_k - \dot{\mathbf{J}}_k(\mathbf{q}_k, \dot{\mathbf{q}}_k) \dot{\mathbf{q}}_k) + \mathbf{n}_k(\mathbf{q}_k, \dot{\mathbf{q}}_k) + \mathbf{J}_k^T(\mathbf{q}_k) \mathbf{h}_k, \quad (32)$$

where \mathbf{q}_k is the (6×1) vector of joint variables, \mathbf{B}_k is the (6×6) symmetric positive definite inertia matrix, \mathbf{n}_k is the (6×1) vector of Coriolis, centrifugal and gravity torques, and \mathbf{J}_k is the (6×6) (nonsingular) Jacobian matrix. Further in (32), \mathbf{a}_k is a new control input which can be chosen as $\mathbf{a}_k = [\mathbf{a}_{p,k}^T \ \mathbf{a}_{\epsilon,k}^T]^T$ where $\mathbf{a}_{p,k}$ and $\mathbf{a}_{\epsilon,k}$ are designed so as to ensure tracking of $\mathbf{p}_{r,k}$ and $\mathcal{Q}_{r,k}$, as well as of $\mathbf{v}_{r,k}$, i.e.,

$$\mathbf{a}_{p,k} = \ddot{\mathbf{p}}_{r,k} + k_{Vp} \Delta \dot{\mathbf{p}}_{r,kk} + k_{Pp} \Delta \mathbf{p}_{r,kk} \quad (33)$$

$$\mathbf{a}_{\epsilon,k} = \dot{\boldsymbol{\omega}}_{r,k} + k_{V\epsilon} \Delta \boldsymbol{\omega}_{r,kk} + k_{P\epsilon} \mathbf{R}_k^k \boldsymbol{\epsilon}_{r,kk} \quad (34)$$

where $\Delta \mathbf{p}_{r,kk} = \mathbf{p}_{r,k} - \mathbf{p}_k$, ${}^k\boldsymbol{\epsilon}_{r,kk}$ is the vector part of $\mathcal{Q}_{r,kk} = \mathcal{Q}_k^{-1} * \mathcal{Q}_{r,k}$, and $\Delta \boldsymbol{\omega}_{r,kk} = \boldsymbol{\omega}_{r,k} - \boldsymbol{\omega}_k$. It is worth remarking that k_{Vp} , k_{Pp} in (33) and $k_{V\epsilon}$, $k_{P\epsilon}$ in (34) are suitable positive feedback gains characterizing inner position and orientation loops which work as in the scheme of Fig. 1.

5. Experiments

The laboratory setup consists of two industrial robots having a six-revolute-joint anthropomorphic geometry with nonnull shoulder and elbow offsets and non-spherical wrist. One robot is mounted on a sliding track, providing an extra prismatic joint (Fig. 2).

The joints are actuated by brushless motors via gear trains; shaft absolute resolvers provide motor position measurements. Each robot can be controlled either in the standard industrial mode, or in the open mode. In the latter case, the control unit is connected to a PC Pentium, which is in charge of computing the control algorithm and passing the references to the current servos through the communication link at 1 ms sampling time. Joint velocities are reconstructed through numerical differentiation of joint position readings. A

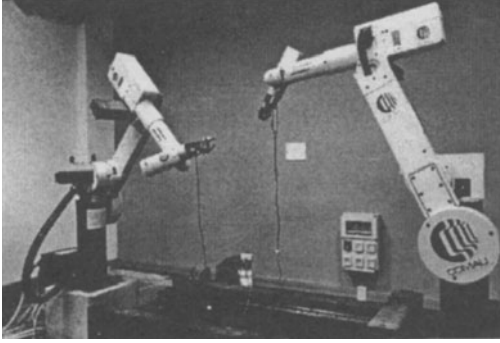


Figure 2: Dual-robot setup available in the lab.

six-axis force/torque sensor ATI FT 130/10 with force range of ± 130 N and torque range of ± 10 Nm is mounted at the wrist of each robot manipulator. The sensors are connected to the PC by parallel interface boards which can provide readings of six components of generalized force at 1 ms.

5.1. Loose cooperation

The first experiment is devoted to testing loose cooperative control for a parts mating task. The seven-joint manipulator is assumed to carry the peg while the six-joint manipulator is assumed to hold the hollow part.

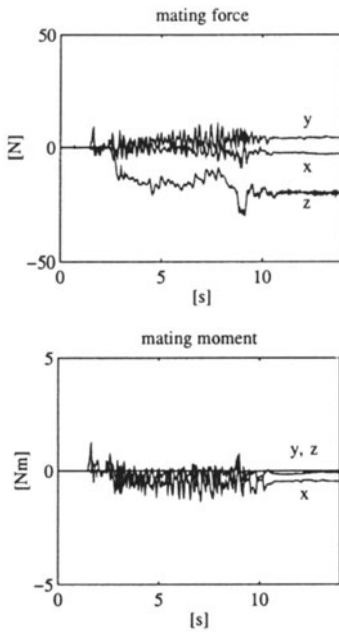


Figure 3: Time history of mating force and moment.

The task is planned on the seven-joint manipulator using the standard industrial control unit. From a given posture a joint space motion is commanded to

reach a suitable intermediate posture which facilitates the subsequent phases of the task. Then, a Cartesian space motion along a straight-line path is commanded to drive the tip of the peg to a position proximal to the mouth of the hole and align the approach axis of the peg with the axis of the hole, as accurately as possible. Finally, a straight-line motion along the approach axis—typically at a reduced speed with respect to the previous phase—is commanded to realize the insertion.

The six-joint manipulator is controlled using the open control mode so that the object (hollow part) behaves as a mechanical impedance; the force/torque sensor is mounted at the wrist.

The peg is a wooden cylinder of 17 mm diameter and 80 mm height, while the other part is a wooden block with a hole of 18 mm diameter and 70 mm depth; that is, a 0.5 mm radial clearance is present during the insertion.

An insertion task is programmed in terms of a planned motion for the seven-joint manipulator requiring a displacement of 90 mm along the end-effector approach axis, so as to get a 20 mm overshoot beyond the bottom of the hole. The proximate location has been chosen so as to introduce an intentional misalignment of 3 deg between the peg and hole axes.

The six-joint manipulator is impedance-controlled so that the origin of Σ_o is located 95 mm beyond the bottom of the hole along its axis. The parameters of the impedance in (2), (10) have been set to $M_p = \text{diag}\{15, 40, 15\}$, $D_p = \text{diag}\{300, 950, 300\}$, $K_p = \text{diag}\{400, 1300, 400\}$ for the translational part, and $M_e = \text{diag}\{9, 9, 9\}$, $D_e = \text{diag}\{13.5, 13.5, 13.5\}$, $K_e = \text{diag}\{1, 1, 1\}$ for the rotational part. The feedback gains in (15), (16) have been set to $k_{V_p} = 70$, $k_{P_p} = 2025$ for the position loop, and $k_{V_e} = 70$, $k_{P_e} = 5000$ for the orientation loop, respectively.

The results are illustrated in Fig. 3 in terms of the time history of the three components of mating force and moment. Remarkably, the values of force and moment keep limited despite of the incorrect task planning. At steady state, residual values of force and moment can be observed which are obviously caused by the planned misalignment and overshoot.

5.2. Tight cooperation

The second experiment is devoted to testing tight cooperative control. The two robot end effectors tightly grasp the ends of a wooden bar of 1 m length. At the center of the bar is fixed a steel stick with a wooden disk of 5.5 cm radius at its tip.

The environment is constituted by a cardboard box; the translational stiffness at the contact between the

disk and the surface is of the order of 5000 N/m, while the rotational stiffness for small angles is of the order of 15 Nm/rad.

The task in the experiment consists in taking the disk in contact with the surface; that is placed at an unknown distance with an angle of unknown magnitude. The origin of Σ_o is required to make a desired motion along a straight line with a vertical displacement of -0.275 m along the Z -axis of Σ_b . The trajectory along the path is generated according to a 5th-order interpolating polynomial with null initial and final velocities and accelerations, and a duration of 6 s. The desired orientation of the object frame is required to remain constant.

The parameters of the translational part of the impedance equation (2) have been set to $M_p = \text{diag}\{30, 30, 30\}$, $D_p = \text{diag}\{555, 555, 555\}$, $K_p = \text{diag}\{1300, 1300, 1300\}$, while the parameters of the rotational part of the impedance equation (10) have been set to $M_e = \text{diag}\{10, 2, 10\}$, $D_e = \text{diag}\{35, 20, 35\}$, $K_e = \text{diag}\{20, 8, 20\}$. Notice that the stiffness matrices have been chosen so as to ensure a compliant behavior (limited values of contact force and moment) during the contact, while the damping matrices have been chosen so as to guarantee a well-damped behavior.

The feedback gains in (33), (34) have been set to $k_{Vp} = 65$, $k_{Pp} = 1800$ for the position loop, and $k_{Ve} = 65$, $k_{Pe} = 3600$ for the orientation loop, respectively. Notice that these values differ from those for the first experiments because the sampling time had to be increased to 2 ms in order to synchronize the two robot control units.

From Fig. 4, after the contact, the component along the Z -axis of the position displacement between the desired frame Σ_d and the object frame Σ_o , expressed in Σ_b , significantly deviates from zero, as expected; a smaller displacement can also be seen for the component along the X -axis, due to contact friction. As for the orientation displacement between Σ_o and Σ_d , expressed in Σ_d , only the component along the Y -axis significantly deviates from zero since the object frame has to rotate about the Y -axis of Σ_d in order to comply with the surface after the contact.

From Fig. 5, in view of the imposed task, a prevailing component of the contact force can be observed along the Z -axis after the contact, while a significant component along the X -axis arises, corresponding to the above position displacement. As for the contact moment, the only nonnegligible component is that along the Y -axis of Σ_d , which corresponds to the above orientation displacement. It can be recognized that all the above quantities reach constant steady-state

values after the desired motion is stopped. The oscillations on the force and moment can be ascribed to the effects of the commonly held object on the measurements.

6. Conclusion and Perspectives

The problem of cooperative manipulation of an object by a dual-robot system has been successfully tackled by resorting to a geometrically consistent impedance control framework where orientation displacements and tracking errors have been expressed in terms of unit quaternions. Experimental validation on a dual-robot industrial setup for a parts mating task and for a task where a tightly grasped object is in contact with a compliant surface has been provided.

The presented results accord with the current trends in the European robotics industry which have featured realization of six-DOF manual devices for intuitive robot programming, resort to model-based dynamic control techniques, and development of open control architectures for on-line sensory feedback. Foreseen developments for industrial setups may include manipulation of flexible objects, integration of visual feedback, and low-cost emulation of manipulation in microgravity, e.g., free-floating robots, free-flying objects.

It is conjectured that future research efforts will also be addressed toward the application of impedance control and cooperative manipulation concepts to haptic devices, interaction control of lightweight and redundant robots, and control of vehicle-manipulator systems.

Acknowledgments

This work was supported by *MURST* and *ASI*.

References

- [1] Hogan, N., 1985, "Impedance control: An approach to manipulation," *ASME J. of Dynamic Systems, Measurement, and Control*, Vol. 107, pp. 1–24.
- [2] Siciliano, B., Villani, L., 2000, *Robot Force Control*, Kluwer, Boston, MA.
- [3] Khatib, O., 1987, "A unified approach for motion and force control of robot manipulators: The operational space formulation," *IEEE J. of Robotics and Automation*, Vol. 3, pp. 43–53.
- [4] Fasse, E.D., Broenink, J.F., 1997, "A spatial impedance controller for robotic manipulation," *IEEE Trans. on Robotics and Automation*, Vol. 13, pp. 546–556.
- [5] Caccavale, F., Natale, C., Siciliano, B., Villani, L., 1999, "Six-DOF impedance control based on an-

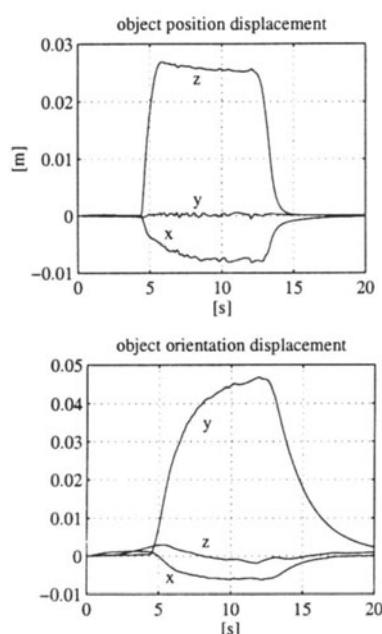


Figure 4: Object position and orientation displacement between Σ_d and Σ_o .

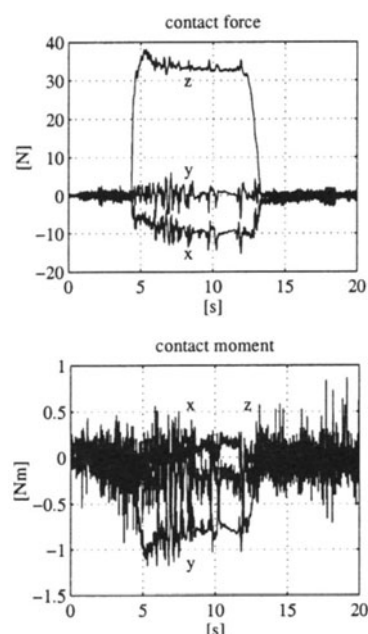


Figure 5: Contact force and moment acting on the object.

- gle/axis representations," *IEEE Trans. on Robotics and Automation*, Vol. 15, pp. 289–300.
- [6] Nakano, E., Ozaki, S., Ishida, T., Kato, I., 1974, "Co-operational control of the anthropomorphic manipulator 'MELARM'," *Proc. 4th Int. Symp. on Industrial Robots*, Tokyo, Japan, pp. 251–260.
- [7] Luh, J.Y.S., Zheng, Y.F., 1987, "Constrained relations between two coordinated industrial robots for motion control," *International Journal of Robotics Research*, Vol. 6, no. 3, pp. 60–70.
- [8] Nakamura, Y., Nagai, K., Yoshikawa, T., 1989, "Dynamics and stability in coordination of multiple robotic mechanisms," *International Journal of Robotics Research*, Vol. 8, no. 2, pp. 44–61.
- [9] Li, Z., Hsu, P., Sastry, S., 1989, "Grasping and coordinated manipulation by a multifingered robot hand," *Int. J. of Robotics Research*, Vol. 8, no. 4, pp. 33–50.
- [10] Uchiyama, M., Dauchez, P., 1993, "Symmetric kinematic formulation and non-master/slave coordinated control of two-arm robots," *Advanced Robotics*, Vol. 7, pp. 361–383.
- [11] Khatib, O., 1995, "Inertial properties in robotic manipulation: an object-level framework," *Int. J. of Robotics Research*, Vol. 14, pp. 19–36.
- [12] Bonitz, R.G., Hsia, T.C., 1996, "Internal force-based impedance control for cooperating manipulators," *IEEE Trans. on Robotics and Automation*, Vol. 12, pp. 78–89.
- [13] Schneider, S.A., Cannon, Jr., R.H., 1992, "Object impedance control for cooperative manipulation: Theory and experimental results," *IEEE Trans. on Robotics and Automation*, Vol. 8, pp. 383–394.
- [14] Khatib, O., Yokoi, K., Chang, K., Ruspini, D., Holmberg, R., Casal, A., 1996, "Coordination and decentralized cooperation of multiple mobile manipulators," *J. of Robotic Systems*, Vol. 13, pp. 755–764.
- [15] Caccavale, F., Siciliano, B., Villani, L., 1999, "Robot impedance control with nondiagonal stiffness," *IEEE Trans. on Automatic Control*, Vol. 44, pp. 1943–1946.
- [16] Whitney, D.E., 1982, "Quasi-static assembly of compliantly supported rigid parts," *ASME J. of Dynamic Systems, Measurement, and Control*, Vol. 104, pp. 65–77.
- [17] Cutkosky, M.R., Wright, P.K., 1986, "Active control of a compliant wrist in manufacturing tasks," *ASME J. of Dynamic Systems, Measurement, and Control*, Vol. 108, pp. 36–43.
- [18] Hollis, R.L., Salcudean, S.E., Allan, A.P., 1991, "A six-degree-of-freedom magnetically levitated variable compliance fine-motion wrist," *IEEE Trans. on Robotics and Automation*, Vol. 7, pp. 320–332.
- [19] Sciavicco, L., Siciliano, B., 1996, *Modelling and Control of Robot Manipulators*, 2nd Ed., Springer-Verlag, London.
- [20] Chou, J.C.K., 1992, "Quaternion kinematic and dynamic differential equations," *IEEE Trans. on Robotics and Automation*, Vol. 8, pp. 53–64.
- [21] Natale, C., Siciliano, B., Villani, L., 1999, "Spatial impedance control of redundant manipulators," in *Proc. 1999 IEEE Int. Conf. on Robotics and Automation*, Detroit, MI, pp. 1788–1793.
- [22] Chiacchio, P., Chiaverini, S., Siciliano, B., 1996, "Direct and inverse kinematics for coordinated motion tasks of a two-manipulator system," *ASME J. of Dynamic Systems, Measurement, and Control*, Vol. 118, pp. 691–697.